Treated *Nypa fruticans* Husk-filled Regenerated Cellulose Biocomposite Films

Vaniespree Govindan,* Salmah Husseinsyah, and Teh Pei Leng

The effects of filler content and methacrylate acid (MAA) treated *Nypa fruticans* husk (NFH) on the mechanical properties, X-ray diffraction (XRD), thermogravimetric analysis (TGA), and morphology of NFH regenerated cellulose (RC) biocomposite films were investigated. Ionic liquid containing 8 wt% of lithium chloride (LiCl)/N,N-dimethylacetamide (DMAc) was used to dissolve microcrystalline cellulose (MCC) and NFH to produce NFH RC biocomposite films. Methacrylate acid was used as a modifying agent on the NFH to promote better mechanical and thermal properties for the resulting NFH RC biocomposite films. The results showed that the tensile strength, Young's modulus, crystallinity index (CrI), moisture content, and thermal stability of the untreated NFH RC biocomposite films increased with increasing NFH content up to 3 wt% and decreased with further increments. The MAA-treated NFH showed improved tensile strength and Young's modulus compared with the untreated NFH RC biocomposite films. The presence of MAA enhanced the crystallinity index (CrI), moisture resistance, and thermal stability of the NFH RC biocomposite films. Good interfacial interaction between the NFH and RC matrix was proven by scanning electron microscopy (SEM).

Keywords: Nypa fruticans husk; Microcrystalline Cellulose; Regenerated cellulose; Biocomposite films; Methacrylic acid

*Contact information: Division of Polymer Engineering, School of Materials Engineering, Universiti Malaysia Perlis, 02600, Jejawi, Perlis, Malaysia; *Corresponding author: vaniespree89@yahoo.com*

INTRODUCTION

Cellulose appears to be one of the most promising molecules in addressing the depletion of non-renewable resources and fossil fuel-based polymer materials (Clark 2007; Simkovic 2008). Cellulose demonstrates a number of advantageous properties such as renewability and biodegradability (Chen *et al.* 2011), high specific strength and stiffness (Klemm *et al.* 2005; Zimmermann *et al.* 2010; Afra *et al.* 2013), large specific surface area, and high reinforcing potential (Abraham *et al.* 2011). Dissolution and processing of cellulose, however, is difficult in general because of its large proportion of intra- and intermolecular hydrogen bonds (Cai and Zhang 2006) and its partially crystalline structure, which causes it to be neither meltable nor soluble in conventional solvents (Park *et al.* 2004; Ruan *et al.* 2004).

Recently, a new type of solvent, namely ionic liquids (ILs), which are considered green solvents, has been reported to be an effective and promising cellulose solvent (Zhang *et al.* 2005; Zhu *et al.* 2006; Song *et al.* 2013). Ionic liquids have the potential to be eco-friendly with characteristics of low melting point, non-volatility, thermal stability, low flammability, non-explosiveness, ease of recycling, good recoverability, and superior dissolving capacity (Rahatekar *et al.* 2009; Zhang *et al.* 2010; Mahmoudian *et al.* 2012). Typical examples of ILs include lithium chloride (LiCl)/N,N-dimethylacetamide (DMAc),

1-butyl-3-methylimidazolium chloride ([BIM][Cl]), N-methylmorpholine N-oxide (NMMO), 1-ethyl-3-methylimidazolium acetate ([Emim][Ac]), and 1-n-allyl-3-methylimidazolium chloride ([Amim][Cl]) (Shafiei *et al.* 2013; Soheilmoghaddam *et al.* 2013; Olsson *et al.* 2014).

During preparation of regenerated cellulose, the surface layer of the cellulose is partially dissolved to form the matrix phase of a biocomposite. Meanwhile, the remaining cell cores maintain their original structure and impart a reinforcing effect on the biocomposite. This constitutes a simplified biocomposite preparation process while improving the filler/matrix interface. All-cellulose composites resulting from this process have shown excellent mechanical properties similar to or better than those prepared by a traditional impregnation method (Gindl and Keckes 2005; Nishino and Arimoto 2007; Soykeabkaew *et al.* 2009).

Nypa fruticans is a species of palm that grows liberally and can be found consistently throughout Malaysia. *Nypa fruticans* husk (NFH) consists of 28.8 to 45.7 wt% cellulose, 21.8 to 26.4 wt% hemicellulose, and 19.4 to 33.8 wt% lignin (La Mantia and Morreale 2001). *Nypa* is a favorable source in various applications because of its high content of cellulose. It is known that the presence of lignin in natural fillers leads to poor mechanical properties in regenerated cellulose. Interfacial adhesion between filler and matrix can be improved by promoting surface modification on the filler and thus enhancing the mechanical properties of resulting biocomposite films (Hahary *et al.* 2015; Zailuddin *et al.* 2015). The hydrophilic nature of the filler also can be reduced *via* filler modification to enhance the filler dispersion, wettability and filler-matrix interaction (Park *et al.* 2008).

This work's precursor studies (Govindan *et al.* 2014, 2015) reported on the effect of microcrystalline cellulose (MCC) and NFH contents on the properties of NFH regenerated cellulose (RC) biocomposite films. In the present study, methacrylic acid (MAA) was used to modify the NFH to improve the properties of NFH RC biocomposite films. The effects of NFH content and MAA on the biocomposite films's tensile properties, X-ray diffraction (XRD), thermogravimetric analysis (TGA), and morphology were studied.

EXPERIMENTAL

Materials

Nypa fruticans husk (NFH) was obtained from a plantation at Kuala Perlis, Malaysia. The husks were cleaned and grounded into particle sizes of 36 µm before further use. N, N-dimethylacetamide (DMAc) and lithium chloride (LiCl) were purchased from Across (Belgium). Sodium chlorite, microcrystalline cellulose (MCC), and acetone were supplied by Sigma-Aldrich (USA). Acetic acid was obtained from BASF (Germany). Sodium hydroxide (NaOH) and sulfuric acid (H_2SO_4) were supplied by HmbG Chemical (Germany). Methacrylic acid was purchased from Aldrich Chemical Company, Inc. (USA).

Pretreatment of Filler (Untreated NFH)

The NFH was prepared by acid hydrolysis using sulfuric acid. The NFH were first heated in 2% NaOH solution at 80 °C to remove the lignin. Bleaching treatment was proceeded by heating the NFH in 30% $NaClO_2$ and a few drops of glacial acetic acid at 70 °C for 1 h. This bleaching procedure was repeated three times using the same conditions.

Next, acid hydrolysis was conducted with 64% sulfuric acid at 45 °C with a fiber-to-acid ratio of 1:10 (g/mL) for 45 min, followed by filtration and washing with distilled water until a neutral pH was achieved. Finally, the NFH was dried in an oven at 80 °C for 3 h.

Chemical Modification (Treated NFH)

The methacrylic acid (MAA) was first dissolved in ethanol (3% (v/v)). The pre-treated NFH was then slowly added into the MAA solution, and the mixture was stirred for 2 h. The NFH was later filtered and dried in an oven at 80 °C.

Preparation of NFH RC Biocomposite Films

For each experiment, the MCC was activated to swell the cellulose structure. The activation of the cellulose was carried out as follows: swelling of the MCC in distilled water, filtering, solvent exchange (twice in acetone followed by DMAc for 40 min each), and drying at 80 °C for 3 h. *Nypa fruticans* husk regenerated cellulose (NFH RC) biocomposite films were prepared by dissolving 3 wt% MCC and various contents of untreated and treated NFH (1, 2, 3, and 4 wt%) in 8 wt% LiCl/DMAc solution at room temperature for 30 min with the aid of agitation until a homogeneous solution was generated. The NFH RC biocomposite films were washed using distilled water for 30 min to remove the excess DMAC/LiCl co-solvent and then dried at room temperature for 24 h. The formulations of the treated and untreated NFH RC biocomposite films are listed in Table 1.

Table 1. Formulations of Untreated and Treated NFH RC Biocomposite Films

Materials	Untreated NFH RC Biocomposite Films	MAA-Treated NFH RC Biocomposite Films
MCC (wt%)	3	3
NFH (wt%)	1, 2, 3, 4	1, 2, 3, 4
MAA (%)*	-	3
*3% based on weight of NFH		

Tensile Testing

Tensile properties (tensile strength, elongation at break, and Young's modulus) of the NFH RC biocomposite films were determined using an Instron universal testing machine model 5569 according to ASTM D882-12 (2012). Specimens of 15 mm x 100 mm were cut and used in tensile testing. Ten samples were prepared for each composition. A cross-head speed of 10 mm/min was used, and the tests were conducted at 25 ± 3 °C and relative humidity (RH) of 50 ± 2%.

X-Ray Diffraction (XRD)

The crystallinity index of untreated and NFH RC biocomposite films treated with MAA were evaluated using a Bruker D8 Advance diffractometer (USA). The XRD pattern was obtained using a diffractometer equipped with an X-ray tube with Cu-Kα (λ=1.5418A°) radiation under normal atmospheric conditions at room temperature in a scan range of 2° to 40°. The crystallinity index (CrI) was calculated using Eq. 1, where I represents the maximum intensity of the (002) lattice peak and I' is the maximum intensity of the amorphous material.

$$\text{Crystallinity Index (CrI)} = 100\ (I - I') / I \quad (1)$$

Scanning Electron Microscopy (SEM)

A scanning electron microscope (SEM) model JEOL (USA) at a voltage of 5 kV was used to analyze the tensile fracture surface of the NFH RC biocomposite films. The samples were sputter coated with a thin layer of palladium prior to testing.

Fourier Transmission Infrared (FTIR)

FTIR was used to determine the chemical functional group of NFH RC biocomposite films. A Perkin Elmer, Model L1280044 instrument was used to performed FTIR analysis. The attenuated total reflectance (ATF) method was used. The samples were recorded at the range of 4000 to 600 cm^{-1} with a resolution of 4 cm^{-1}.

Thermogravimetric Analysis (TGA)

Thermogravimetric analysis was used to measure the weight loss and thermal stability in the NFH RC biocomposite films as a function of temperature in a controlled atmosphere. The thermal properties of the NFH RC biocomposite films were determined using a TGA Pyris Diamond, Perkin-Elmer (USA). Ten milligrams of each specimen was individually placed into a platinum crucible and heated from 30 to 600 °C at a rate of 10 °C/min with a nitrogen gas flow of 50 mL/min.

Moisture Content

To prepare for moisture content testing, samples with dimension of 20 mm x 15 mm were weighed at room conditions. They were then dried in an oven at 105 °C for 24 h and weighed again. Three weight loss measurements were recorded for each formulation ratio. The moisture content of the NFH RC biocomposite films was then calculated using Eq. 2,

$$\text{Moisture content } (\%) = \frac{Wo - W1}{W1} \text{ x } 100\% \quad (2)$$

where *Wo* is the weight of the NFH RC biocomposite films before drying and W_1 is the weight of the dried NFH RC biocomposite films.

Mathematical Models for Particulate Reinforced Composites

Nicolais-Narkis Model

The interaction between the filler and the matrix in the biocomposite films can be predicted using the Nicolais-Narkis equation. This theory was developed to investigate the dependence of the composite properties on the filler content fraction. The theoretical value is calculated based on Eq. 3 (Lavengood *et al.* 1973; Ramaraj 2007),

$$\sigma_c = \sigma_0 (1 - 1.21 \emptyset^{2/3}) \quad (3)$$

where σ_c is the tensile strength of the NFH RC biocomposite film, σ_0 is the tensile strength of the control RC biocomposite film, and $\emptyset$ is the volume fraction of NFH in the biocomposite film.

Nielsen Model

The relationship between the elongation and volume fraction of the filler was clarified using the Nielsen equation. The Nielsen equation also can be used to establish the

interaction between the filler and the matrix, as shown in Eq. 4 (Nielsen 1966; Yeng *et al.* 2015).

$$\varepsilon_c = \varepsilon_0 (1- \emptyset^{1/3}) \quad (4)$$

where ε_c is the elongation at break of the polymer composite and ε_0 is the elongation at break of the polymer matrix.

RESULTS AND DISCUSSION

Tensile Properties

Figure 1 shows the tensile strength of the untreated and MAA-treated RC biocomposite films at various NFH contents. The tensile strength of both untreated and treated NFH RC biocomposite films increased significantly until 3 wt% NFH and then decreased at 4 wt%. The decrease in tensile strength is attributed to the agglomeration of NFH. It should also be noted that the tensile strengths of the treated NFH RC biocomposite films were higher than those of the untreated NFH RC biocomposite films at the same NFH content. This improvement in tensile strength was due to better interfacial adhesion between the filler-matrix interfaces, which caused better stress transfer from the matrix to the filler. This is attributed to the hydroxyl group of NFH reacting with the methacrylate of MAA through an esterification reaction.

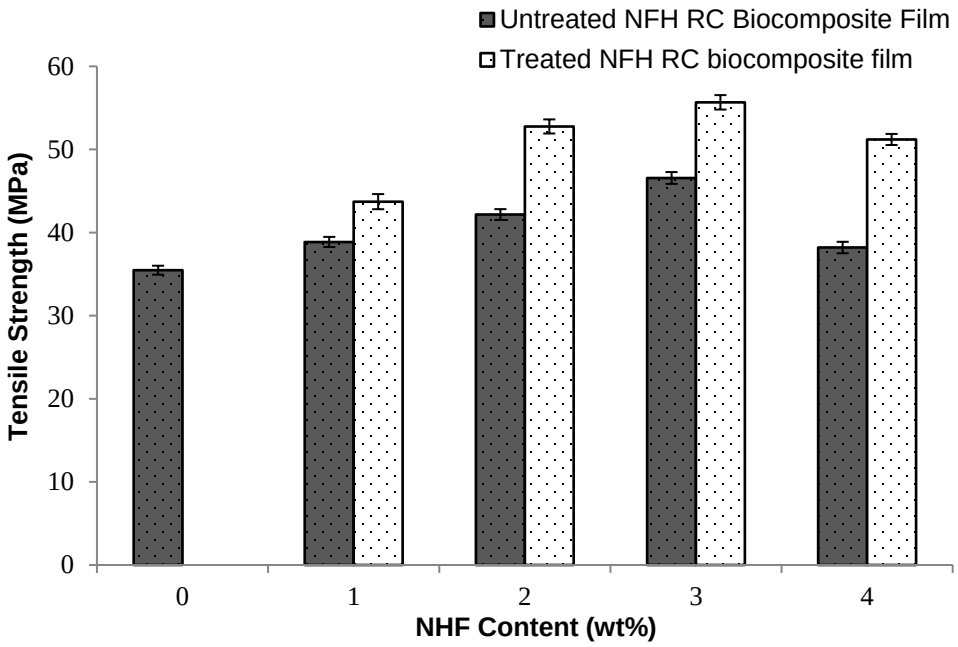

Fig. 1. Effect of NFH content on tensile strength of untreated and MAA-treated NFH RC biocomposite films

Figure 2 shows the relative tensile strength of the experimental and theoretical results that predicted by using Nicolais-Narkis equation (Eq. 3). The Nicolais-Narkis equation is used to indicate the effectiveness of the interaction between filler and matrix with and without the presence of chemical treatment. It can be seen that the relative tensile

strength of theoretical NFH RC biocomposite films decreased linearly as the NFH content increased. However, the experimental tensile strength of treated NFH RC biocomposite films displayed higher values than the predicted and untreated NFH RC biocomposite films. This indicates that the presence of NFH provided the adhesion between the NFH and the RC. Consequently, this model proved that the MAA was successfully deposited on the NFH surface, which enhanced the interfacial adhesion of the NFH RC biocomposite films after modification in agreement with the good dispersion showed in SEM micrograph. Thus, the presence of MAA improved the tensile strength of the NFH RC biocomposite films.

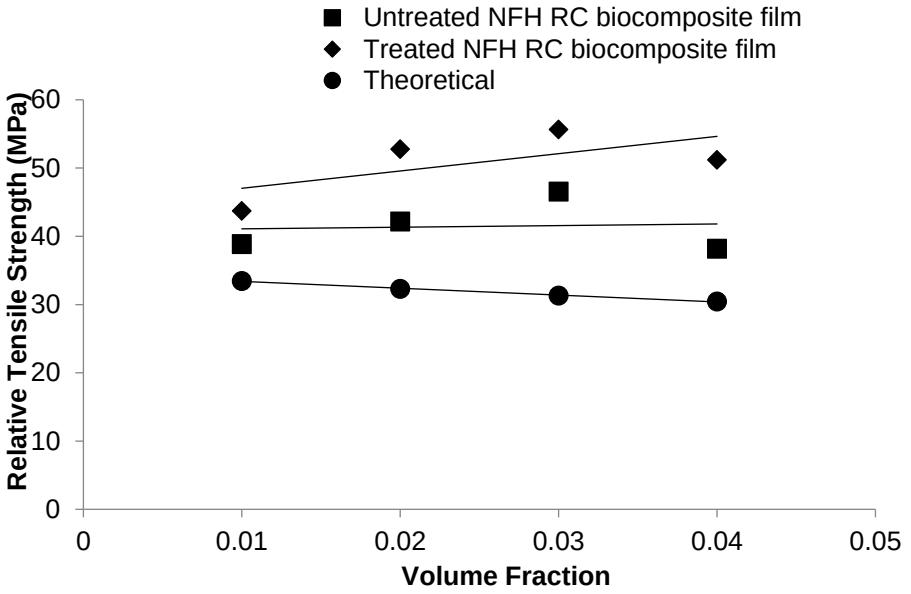

Fig. 2. Relative tensile strength results of theoretical, untreated, and MAA-treated NFH RC biocomposite films

Figure 3 shows the effect of NFH content on the elongation at break of the untreated and MAA-treated NFH RC biocomposite films. The elongation at break for the untreated NFH RC biocomposite films slightly decreased with increasing NFH content. The decrease in elongation at break was caused by the presence of rigid treated NFH particles that inhibited the mobility of the RC chain, resulting in more brittle biocomposite films.

Ma *et al.* (2011) reported a similar trend, wherein the elongation at break of all cellulose nanocomposite decreased as the native cellulose nanofibrils content increased. The treated NFH RC bicomposite films, however, exhibited higher elongation at break properties compared to the untreated NFH RC biocomposite films. The presence of MAA offered strong interfacial bonding between filler and matrix.

Figure 4 displays the relative elongation at break of the experimental and theoretical results that predicted by using Nielsen model (Eq. 4). Both the untreated and treated NFH RC biocomposite films exhibited higher elongation at break values compared to the theoretical NFH RC biocomposite films. Incorporation of NFH into the RC biocomposite films increased the elongation at break compared to the predicted. However, as the volume fraction of NFH increased, the elongation at break decreased, which is equivalent to Nielsen's theory. Besides, the treated NFH RC biocomposite films exhibit highest value due to greater adhesion of the filler to the matrix.

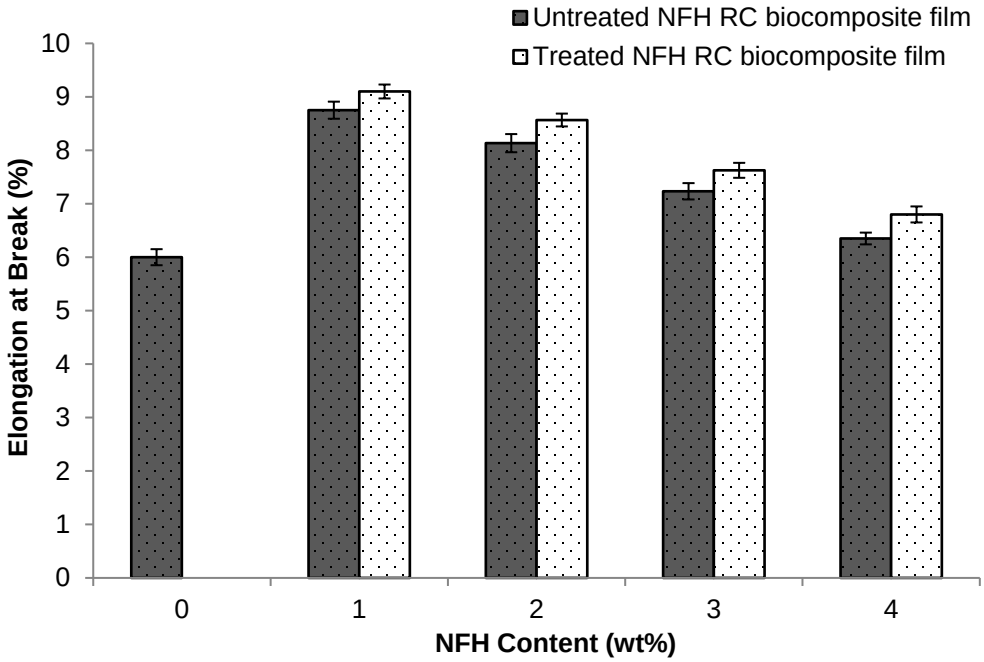

Fig. 3. Effect of NFH content on elongation of break of untreated and MAA treated NFH RC biocomposite films

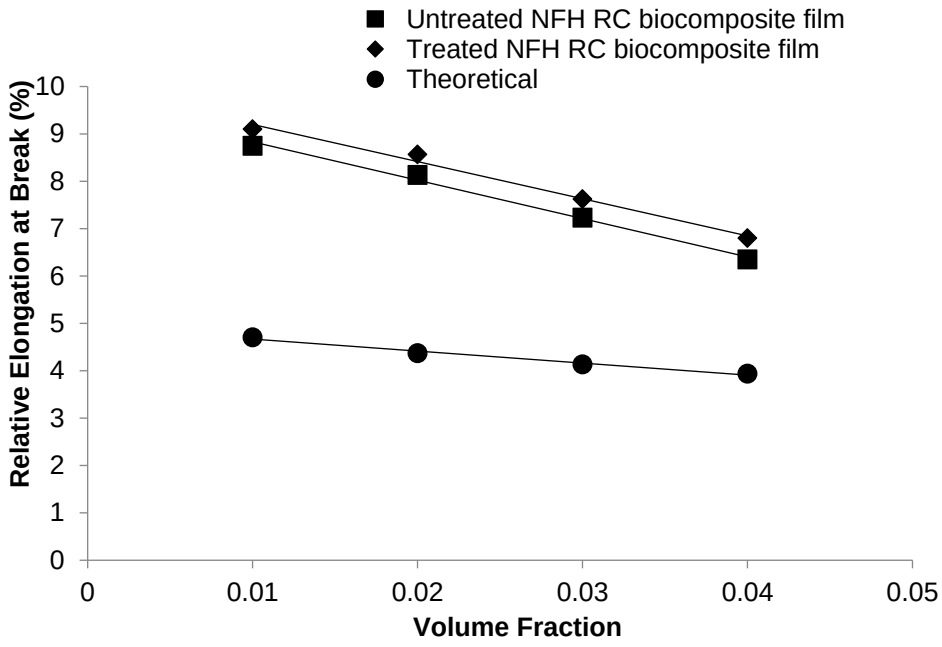

Fig. 4. Relative elongation at break results of theoretical, untreated and MAA-treated NFH RC biocomposite films

The effect of NFH content on the Young's modulus of the untreated and MAA treated NFH RC biocomposite films is shown in Fig. 5. The Young's modulus of the untreated NFH RC biocomposite films showed an increasing trend until 3 wt% NFH; thereafter, at 4 wt%, the Young's modulus decreased. An increase in Young's modulus

with increasing NFH content can be explained by increased in hydrogen bonding, leading to a stiffening effect and high crystallinity index of the NFH RC biocomposite films. A similar result has been observed in the study of poly-(vinyl alcohol) nanocomposites reinforced with cellulose fibrils isolated by high intensity ultrasonication (Cheng *et al.* 2009). Nevertheless, the Young's modulus of the treated NFH RC biocomposite films was higher than that of the untreated NFH RC biocomposite films. The improvement in filler dispersion increased the surface area of the filler-matrix interaction, enhanced interfacial bonding and a stiffening effect was imposed on the NFH RC biocomposite films. The stiffness of the NFH RC biocomposite films increased because the MAA treatment improved the adhesion between the NFH and the RC in the biocomposite films.

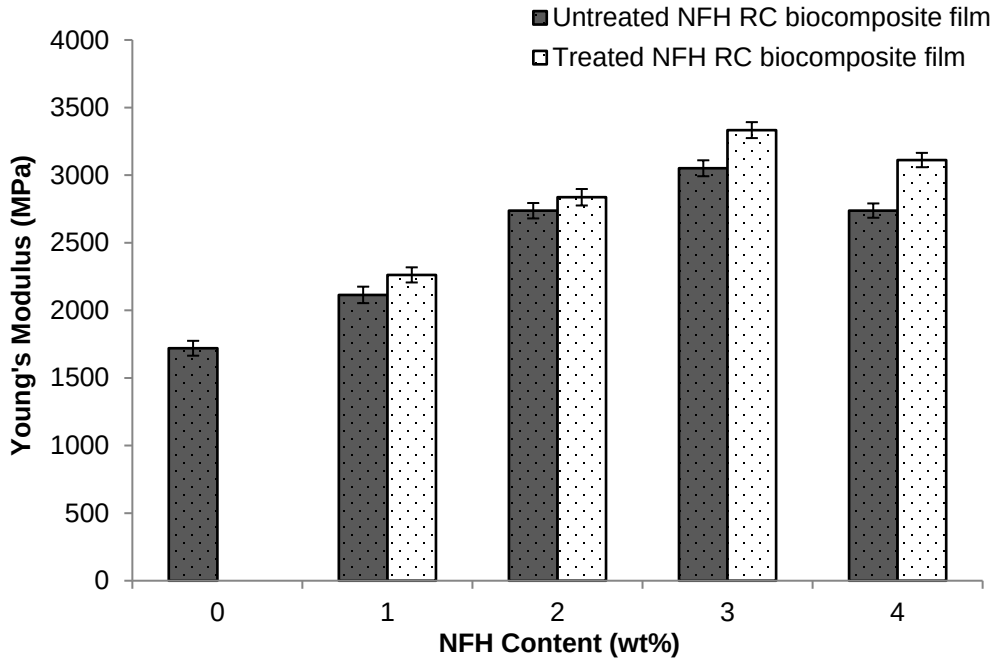

Fig. 5. Effect of NFH content on Young's modulus of untreated and MAA-treated NFH RC biocomposite films

X-Ray Diffraction Analysis

The XRD curves of untreated and MAA-treated NFH RC biocomposite films with various NFH contents are shown in Fig. 6. The crystallinity index (CrI) of the untreated and MAA treated NFH RC biocomposite films at various NFH contents is provided in Table 2.

The addition of NFH to the RC biocomposite increased the CrI. The increment in CrI was attributed to the increase in the stiffness of the untreated NFH RC biocomposite films. This result is parallel to the Young's modulus of the NFH RC biocomposite films.

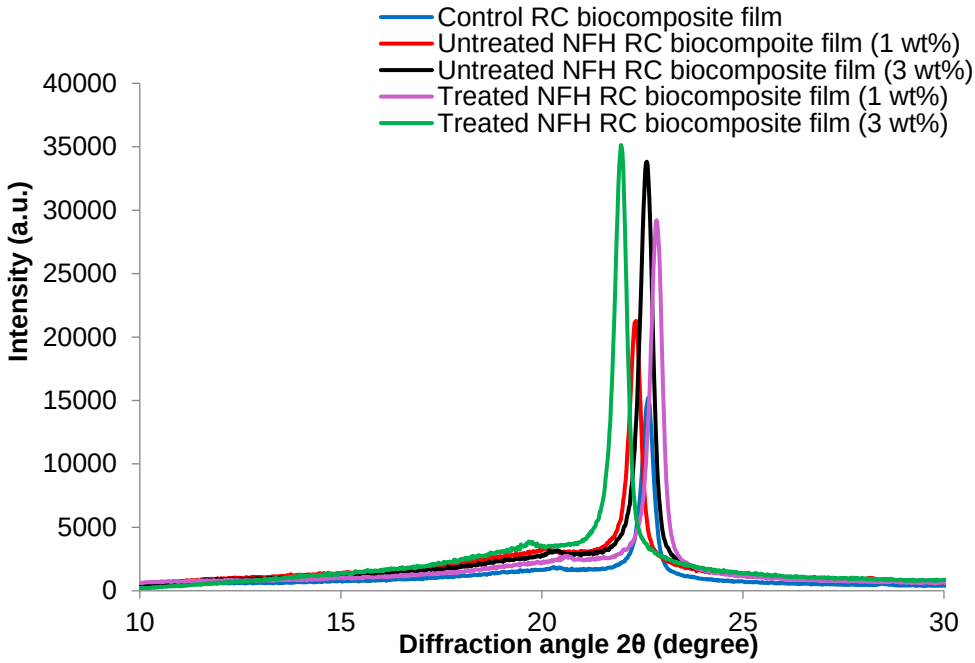

Fig. 6. XRD curves of untreated and MAA-treated NFH RC biocomposite films

The reduction in CrI of the untreated NFH RC biocomposite films at 4 wt% was due to poor dissolution of NFH. Qi *et al.* (2009) found a similar result, decrease in the crystallinity of the films prompt by the increasing cellulose nanofibrils which led to the aggregation and phase separation. The peak result of the treated NFH RC biocomposite films was higher than that of the untreated NFH RC biocomposite films at the same NFH content.

Table 2 shows that the CrI of the treated NFH RC biocomposite films increased with increasing NFH content until 3 wt%; additionally, the CrI of the treated NFH RC biocomposite films was higher than that of the untreated NFH RC biocomposite films. The modification of NFH led to better adhesion and interaction between the NFH and the regenerated cellulose matrix. This can be attributed to an improved nucleating effect of NFH particles, which increased the crystallinity of the treated NFH RC biocomposite films. According to Mohanty et al. (2014) chemically treated fibers shows higher crystallinity than that of the untreated fibers.

Table 2. Crystallinity Index (CrI) of Untreated and MAA-Treated NFH RC Biocomposite Films

RC Biocomposite Film (wt %)	Crystallinity Index (CrI; %)	
	Untreated	MAA treated
Control NFH RC biocomposite film	52.40	52.40
NFH RC biocomposite film 1 wt%	64.87	67.25
NFH RC biocomposite film 2 wt%	67.29	70.09
NFH RC biocomposite film 3 wt%	71.90	73.94
NFH RC biocomposite film 4 wt%	69.51	71.93

Morphology Study

Figure 7 illustrates the SEM tensile fracture surfaces of the untreated and MAA-treated NFH RC biocomposite films at 1 and 3 wt% NFH contents. The micrograph of the untreated NFH RC biocomposite films at 1 wt% is shown in Fig. 7(a).

The micrographs reveal the dispersion of NFH in the RC biocomposite films with the presence of agglomeration; however, at 3 wt% NFH, the micrograph of the untreated NFH RC biocomposite films shows better dispersion, with the presence of fewer voids. On the other hand, both micrographs of the treated NFH RC biocomposite films showed better NFH wettability with the regenerated cellulose matrix as compared to the untreated NFH RC biocomposite films, as shown in Figs. 7 (c) and (d).

At 3 wt% NFH, the treated RC biocomposite films exhibited a smooth surface. The treatment of MAA on the NFH surface attributed to the enhanced interfacial interaction between the NFH and the MAA in the biocomposite films. Furthermore, the enhancement of interfacial adhesion in the MAA treated NFH RC biocomposite films was confirmed by the Nicolais-Narkis and Nielsen equations.

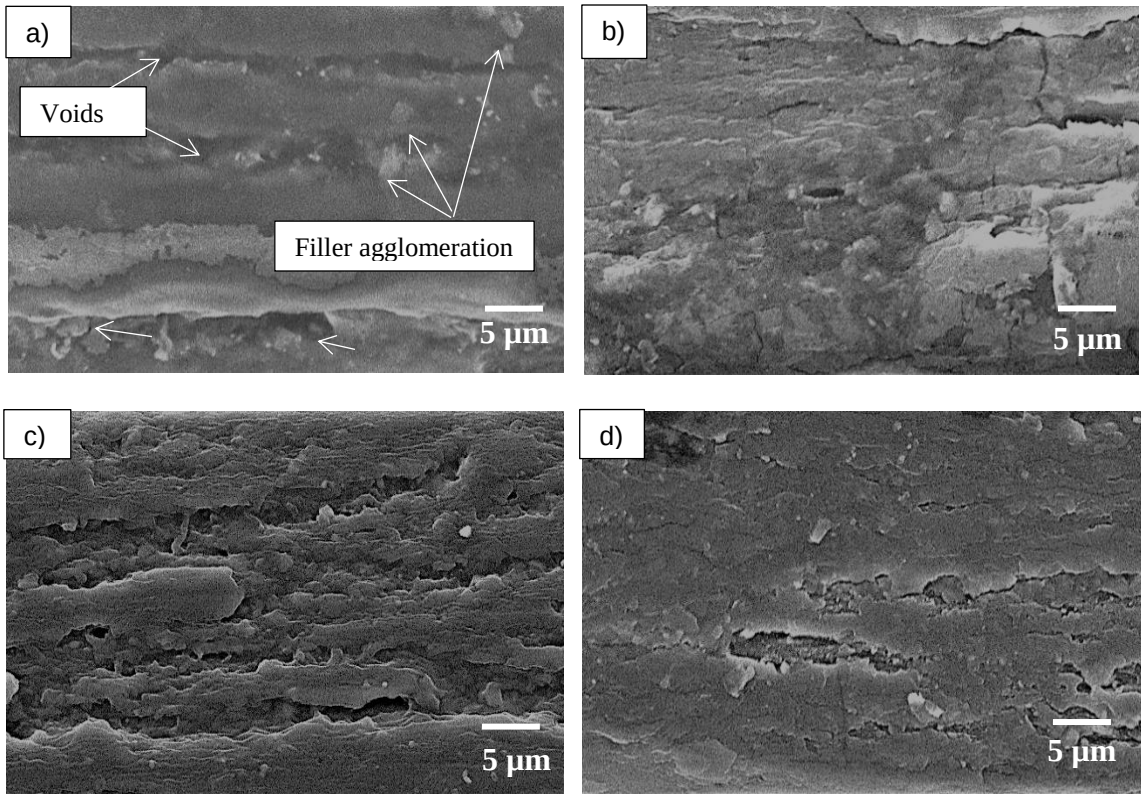

Fig. 7. SEM micrographs of the tensile surface fracture of NFH RC biocomposite films: (a) untreated NFH RC biocomposite film (1 wt%); (b) untreated NFH RC biocomposite film (3 wt%); (c) MAA-treated NFH RC biocomposite film (1 wt%); and (d) MAA-treated NFH RC biocomposite film (3 wt%)

Fourier Transform Infrared Spectroscopy Analysis

Figure 8 shows the FTIR spectra for untreated NFH RC biocomposite film and MAA-treated NFH RC biocomposite film. The peak at 3363 cm^{-1} for untreated NFH RC biocomposite film was due to O-H stretching vibrations gave information concerning the hydrogen bonds. The band at 2800 cm^{-1} to 2960 cm^{-1} for the untreated NFH RC

biocomposite film corresponded to C-H stretching in cellulose II. The appearance of an absorption band at 2299 cm^{-1} is attributed to the C-H stretching of untreated NFH RC biocomposite film. The sharp peak at 1726 cm^{-1} for untreated NFH RC biocomposite film represent the carbonyl (C=O) stretching of cellulose. The peak 1636 cm^{-1} and 1535 cm^{-1} of untreated NFH RC biocomposite film refers to C-O stretching vibration of C-O-H groups and vibration of C=C due to the presence of lignin. The peak 1465 cm^{-1}exhibit by untreated NFH RC biocomposite film is attributed by the mixture of amorphous cellulose and crystallized cellulose II. Furthermore, the peak at 1381 cm^{-1} for untreated NFH RC biocomposite film was attributed by bending vibration of CH_3 groups. The sharp characteristic peak appearing at 1275 cm^{-1} for untreated NFH RC biocomposite film is the stretching vibration of C-O bond. The band at 1099 cm^{-1} was attributed to the C-O bond stretching vibration of C-O-C group in the anhydroglucose ring of cellulose. The appearance of an absorption band at 991 cm^{-1} corresponds to the glycosidic C-H deformation with ring vibration contribution and O-H bending.

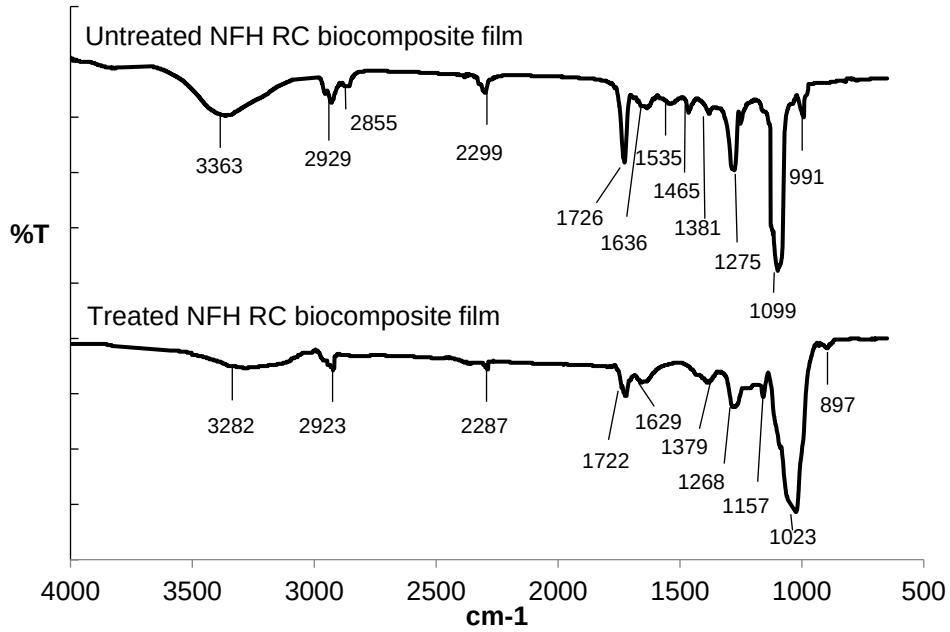

Fig. 8. FTIR spectra of untreated and MAA-treated NFH RC biocomposite films

MAA-treated NFH RC biocomposite film showed a reduction of the peak intensity at 3282 cm^{-1} which is attributed to the reduction of hydrophilicity. Reduction in peak intensity at 2287 cm^{-1} and 2800 to 2960 cm^{-1} corresponded to overlapping of C-H stretching in cellulose II and MAA.

The intensity of peak 1726 cm^{-1} for untreated NFH RC biocomposite was reduced and shifted to 1722 cm^{-1} due to overlapping of carboxyl groups of NFH with C=O of ester bonding between NFH and MAA. The reduction at peak intensity of 1636 cm^{-1}, 1535 cm^{-1} and 1465 cm^{-1} for treated NFH RC biocomposite film which was attributed to the C-O, C=C, and CH_3 was reduced after the treatment with MAA.

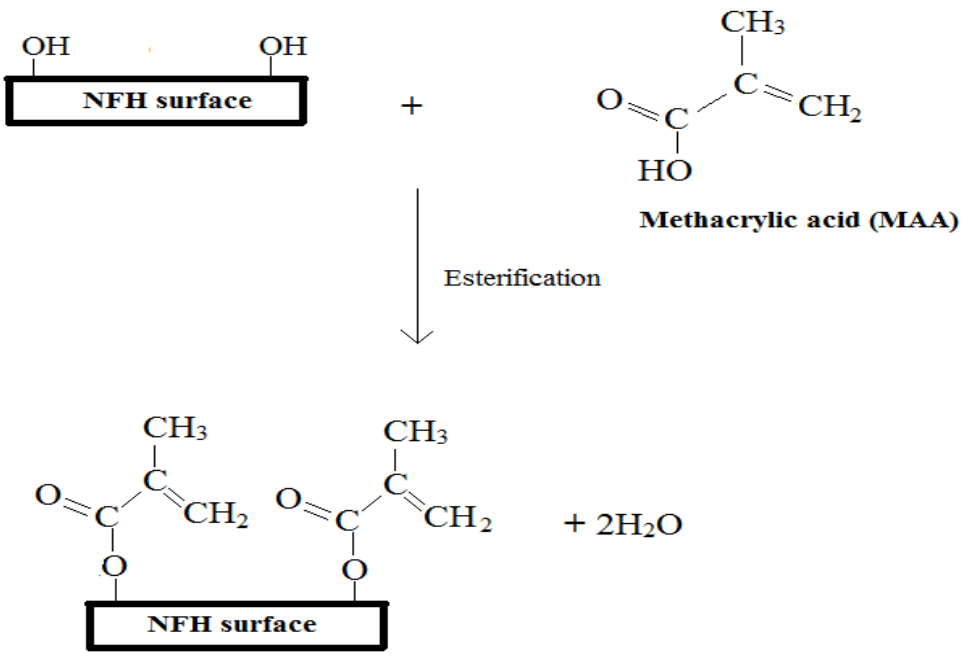

Fig. 9. Schematic reaction of NFH with MAA

There was a breakage of C-O bond during the removal of water after the esterification reaction, which is indicated by the cleavage of 1157 cm^{-1} for C-O group, indicating the bonding between the NFH and the MAA. The intensity of peak situated at 1023 cm^{-1} decreased as the overlapping of C-O groups tends to happened. Besides, the intensity of peak 897 cm^{-1} which referred to C-H deformation and O-H bending was reduced with the presence of the MAA treatment. The schematic reaction of NFH with MAA illustrated in Fig. 9.

Thermogravimetric Analysis

Figure 10 presents the thermogravimetric analysis (TGA) curves of untreated and MAA-treated NFH RC biocomposite films. The TGA data for the films are tabulated in Table 3. The T_{dmax} of the untreated NFH RC biocomposite films increased as the NFH content increased, indicating that the decomposition temperature of the NFH RC biocomposite films was affected by the presence of NFH. Increasing the NFH content increased the formation of pyrolysis material, which acted as a shield and delayed the thermal decomposition of the NFH RC biocomposite films. The weight loss of the untreated NFH RC biocomposite films at T_{300} and T_{600} decreased as the NFH content increased. The lower weight loss denoted higher degradation temperature for the NFH RC biocomposite films. It can be seen that the T_{dmax} of the treated NFH RC biocomposite films was higher than those of the untreated NFH RC biocomposite films. At the same NFH content, the weight loss of the treated NFH RC biocomposite films at T_{300} and T_{600} was lower than that of the untreated NFH RC biocomposite films. The treated NFH RC biocomposite films show higher residue compared to the untreated NFH RC biocomposite films. This reveals that the modification of the NFH surface by MAA improved the thermal stability of the NFH RC biocomposite films. This improvement of thermal stability is due to stronger interaction between the NFH and the matrix.

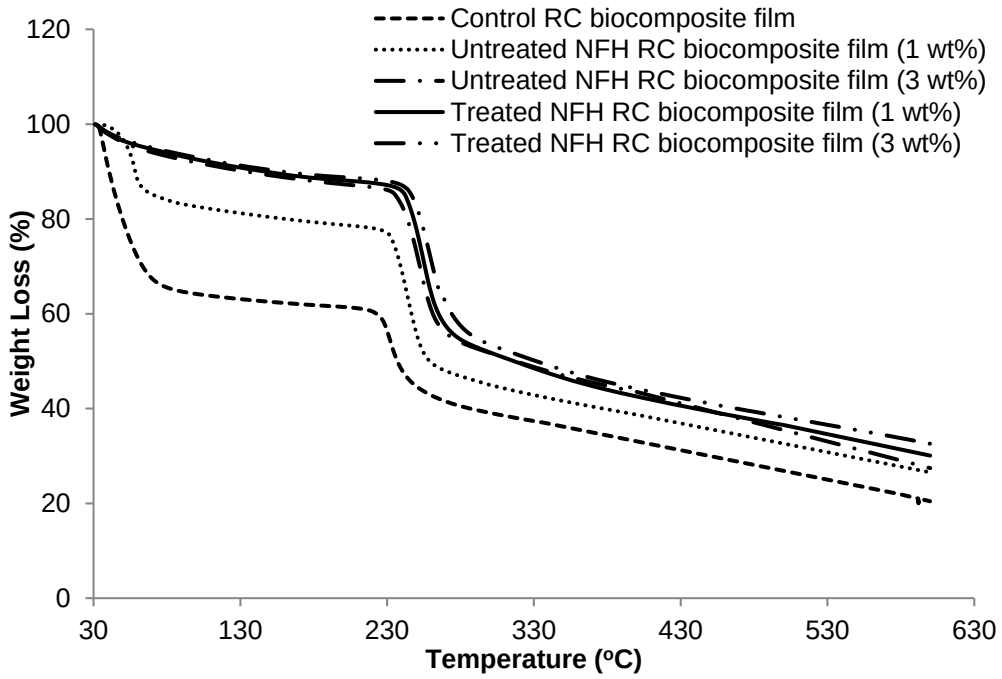

Fig. 10. TGA curves of the untreated and MAA-treated NFH RC biocomposite films

Table 3. TGA Data for Untreated and MAA-Treated NFH RC Biocomposite Films

RC Biocomposite Film (wt %)	T_{dmax} (°C)	Weight Loss (%)		Residue (%)
		300 °C	600 °C	
Control NFH RC biocomposite film	231	58.396	78.706	21.294
Untreated NFH RC biocomposite film 1 wt%	243	50.662	73.458	26.542
Untreated NFH RC biocomposite film 3 wt%	249	49.672	72.558	27.442
Treated NFH RC biocomposite film 1 wt%	254	48.139	69.925	30.075
Treated NFH RC biocomposite film 3 wt%	256	44.957	67.408	32.592

Moisture Content

The moisture content of untreated and MAA-treated NFH RC biocomposite films is illustrated in Fig. 11. The results show that as the NFH content increased, the moisture content of the untreated NFH RC biocomposite films increased. This phenomenon is caused by the presence of plenty of hydroxyl groups on the cellulose surface itself, permitting the reaction between the hydrophilic group of the NFH and water molecules to form hydrogen bonds. Nevertheless, the treated NFH RC biocomposite films displayed a lower moisture content compared to the untreated NFH RC biocomposite films. The overall improvement in moisture resistivity of the treated NFH RC biocomposite films was approximately 17.37% greater than that of the untreated NFH RC biocomposite films. Hence, modification of the NFH surface reduced the amount of active hydroxyl groups that form the hydrogen bonding network with water molecules in the surrounding air.

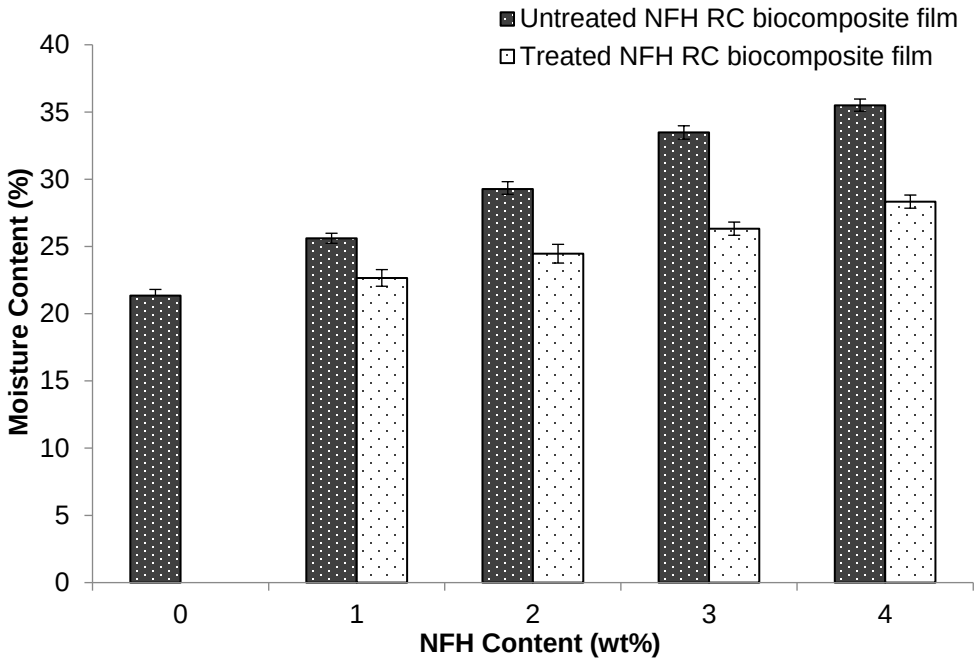

Fig. 11. Moisture content of untreated and MAA-treated NFH RC biocomposite films

CONCLUSIONS

1. The tensile strength, Young's modulus, and crystallinity index of *Nypa fruticans* husk (NFH) regenerated cellulose (RC) biocomposite films increased with increasing NFH content up to 3 wt% and decreased with further addition (4 wt%) of NFH.
2. The thermal stability and moisture content increased as the NFH content increased.
3. The elongation at break of the untreated NFH RC biocomposite films decreased with increasing NFH content.
4. The methacrylic acid (MAA) treatment enhanced the tensile strength, Young's modulus, and crystallinity index of the NFH RC biocomposite films.
5. The treated NFH RC biocomposite films had lower elongation at break values compared to the untreated NFH RC biocomposite films.
6. The treated NFH RC biocomposite films exhibited better thermal stability and moisture resistance than the untreated NFH RC biocomposite films.
7. The SEM micrographs of the tensile fracture surface of the MAA-treated NFH RC biocomposite films showed enhanced dispersion and interfacial interaction between the NFH and the regenerated cellulose matrix compared to the untreated composites.

REFERENCES CITED

Abraham, E., Deepa, B., Pothan, L. A., Jacob, M., Thomas, S., Cvelbar, U., and Anandjiwala, R. (2011). "Extraction of nanocellulose fibrils from lignocellulosic fibres: A novel approach," *Carbohydr. Polym*. 86(4), 1468-1475. DOI: 10.1016/j.carbpol.2011.06.034

Afra, E., Yousefi, H., Hadilam, M. M., and Nishino, T. (2013). "Comparative effect of mechanical beating and nanofibrillation of cellulose on paper properties made from bagasse and softwood pulps," *Carbohydr. Polym*. 97(2), 725-730. DOI: 10.1016/j.carbpol.2013.05.032

ASTM D882-12 (2012). "Standard test method for tensile properties of thin plastic sheeting," ASTM International, West Conshohocken, PA.

Cai, J., and Zhang, L. (2006). "Unique gelation behavior of cellulose in NaOH/urea aqueous solution," *Biomacromolecules* 7(1), 183-189. DOI: 10.1021/bm0505585

Chen, W., Yu, H., Liu, Y., Chen, P., Zhang, M., and Hai, Y. (2011). "Individualization of cellulose nanofibers from wood using high-intensity ultrasonication combined with chemical pretreatments," *Carbohydr. Polym.* 83(4), 1804-1811. DOI: 10.1016/j.carbpol.2010.10.040

Cheng, Q., Wang, S., and Rials, T. G. (2009). "Poly (vinyl alcohol) nanocomposites reinforced with cellulose fibrils isolated by high intensity ultrasonication," *Compos. Pt. A: Appl. Sci. Manufac.* 40(2), 218-224. DOI:10.1016/j.compositesa.2008.11.009

Clark, J. H. (2007). "Green chemistry for the second generation biorefinery—Sustainable chemical manufacturing based on biomass," *J. Chem. Tech. Biotech.* 82(7), 603-609. DOI: 10.1002/jctb.1710

Gindl, W., and Keckes, J. (2005). "All-cellulose nanocomposite," *Polym.* 46(23), 10221-10225. DOI: 10.1016/j.polymer.2005.08.040

Govindan, V., Husseinsyah, S., Leng, T. P., and Amri, F. (2014). "Preparation and characterization of regenerated cellulose using ionic liquid," *Adv. Env. Bio.* 8(8), 2620-2625. DOI: 10.4028/www.scientific.net/amm.754-755.266

Govindan, V., Husseinsyah, S., Leng, T. P., Zakaria, M. M., and Tanjung, F. A. (2015). "Regenerated cellulose/*Nypa fruticans* fiber biocomposite films using ionic liquid," *App. Mech. Mater.* 754, 266-270. DOI: 10.4028/www.scientific.net/amm.754-755.266

Hahary, F. N., Husseinsyah, S., and Zakaria, M. M. (2015). "Improved properties of coconut shell regenerated cellulose biocomposite films using butyl methacrylate," *BioResources* 11(1), 886-898. DOI: 10.15376/biores.11.1.886-898

Klemm, D., Heublein, B., Fink, H. P., and Bohn, A. (2005). "Cellulose: Fascinating biopolymer and sustainable raw material," *Angew. Chem. Int. Ed.* 44(22), 3358-3393. DOI: 10.1002/anie.200460587

La Mantia, F. P., and Morreale, M. (2011). "Green composites: A brief review," *Compos. Pt. A: Appl. Sci. Manufac.* 42(6), 579-588. DOI: 10.1016/j.compositesa.2011.01.017

Lavengood, R. E., Nicolais, L., and Narkis, M. (1973). "A deformational mechanism in particulate-filled glassy polymers," *J. Appl. Polym. Sci.* 17(4), 1173-1185. DOI: 10.1002/app.1973.070170414

Ma, H., Zhou, B., Li, H. S., Li, Y. Q., and Ou, S. Y. (2011). "Green composite films composed of nanocrystalline cellulose and a cellulose matrix regenerated from functionalized ionic liquid solution," *Carbohydr. Polym.* 84(1), 383-389. DOI:10.1016/j.carbpol.2010.11.050

Mahmoudian, S., Wahit, M. U., Ismail, A. F., and Yussuf, A. A. (2012). "Preparation of regenerated cellulose/montmorillonite nanocomposite films *via* ionic liquids," *Carbohydr. Polym.* 88(4), 1251-1257. DOI: 10.1016/j.carbpol.2012.01.088

Mohanty, J. R., Das, S. N., Das, H. C., and Swain, S. K. (2014). "Effect of chemically modified date palm leaf fiber on mechanical, thermal and rheological properties of polyvinylpyrrolidone," *Fibers Polym. 15*(5), 1062-1070. DOI 10.1007/s12221-014-1062-6

Nielsen, L. E. (1966). "Simple theory of stress-strain properties of filled polymers," *J. Appl. Polym. Sci.* 10(1), 97-103. DOI: 10.1002/app.1966.070100107

Nishino, T., and Arimoto, N. (2007). "All-cellulose composite prepared by selective dissolving of fiber surface," *Biomacromolecules* 8(9), 2712-2716. DOI: 10.1021/bm0703416

Olsson, C., Idström, A., Nordstierna, L., and Westman, G. (2014). "Influence of water on swelling and dissolution of cellulose in 1-ethyl-3-methylimidazolium acetate," *Carbohydr. Polym.* 99, 438-446. DOI: 10.1016/j.carbpol.2013.08.042

Park, H. M., Misra, M., Drzal, L. T., and Mohanty, A. K. (2004). "Green nanocomposites from cellulose acetate bioplastic and clay: Effect of eco-friendly triethyl citrate plasticizer," *Biomacromolecules* 5(6), 2281-2288. DOI: 10.1021/bm049690f

Park, J. M., Kim, P. G., Jang, J. H., Wang, Z., Hwang, B. S., and DeVries, K. L. (2008). "Interfacial evaluation and durability of modified Jute fibers/polypropylene (PP) composites using micromechanical test and acoustic emission," *Compos. Pt. B: Eng.* 39(6), 1042-1061. DOI: 10.1016/4j.compositesb.2007.11.00

Qi, H., Cai, J., Zhang, L., and Kuga, S. (2009). "Properties of films composed of cellulose nanowhiskers and a cellulose matrix regenerated from alkali/urea solution," *Biomacromolecules 10(6), 1597-1602*. DOI: 10.1021/bm9001975

Rahatekar, S. S., Rasheed, A., Jain, R., Zammarano, M., Koziol, K. K., Windle, A. H., and Kumar, S. (2009). "Solution spinning of cellulose carbon nanotube composites using room temperature ionic liquids," *Polym.* 50(19), 4577-4583. DOI: 10.1016/j.polymer.2009.07.015

Ramaraj, B. (2007). "Crosslinked poly (vinyl alcohol) and starch composite films. II. Physicomechanical, thermal properties and swelling studies," *J. Appl. Polym. Sci.* 103(2), 909-916. DOI: 10.1002/app.25237

Ruan, D., Zhang, L., Zhou, J., Jin, H., and Chen, H. (2004). "Structure and properties of novel fibers spun from cellulose in NaOH/thiourea aqueous solution," *Macro. Biosc.* 4(12), 1105-1112. DOI: 10.1002/mabi.200400120

Shafiei, M., Zilouei, H., Zamani, A., Taherzadeh, M. J., and Karimi, K. (2013). "Enhancement of ethanol production from spruce wood chips by ionic liquid pretreatment," *Appl. Ener.* 102, 163-169. DOI: 10.1016/j.apenergy.2012.05.060

Simkovic, I. (2008). "What could be greener than composites made from Polysaccharides?," *Carbohydr. Polym.* 74(4), 759-762. DOI: 10.1016/j.carbpol.2008.07.009

Soheilmoghaddam, M., and Wahit, M. U. (2013). "Development of regenerated cellulose/ halloysite nanotube bionanocomposite films with ionic liquid," *Int. J. Bio. Macromol.* 58, 133-139. DOI: 10.1016/j.ijbiomac.2013.03.066

Song, H. Z., Luo, Z. Q., Wang, C. Z., Hao, X. F., and Gao, J. G. (2013). "Preparation and characterization of bionanocomposite fiber based on cellulose and nano-SiO_2 using ionic liquid," *Carbohydr. Polym.* 98(1), 161-167.DOI: 10.1016/j.carbpol.2013.05.079

Soykeabkaew, N., Sian, C., Gea, S., Nishino, T., and Peijs, T. (2009). "All-cellulose nanocomposites by surface selective dissolution of bacterial cellulose," *Cellulose* 16(3), 435-444. DOI: 10.1016/j.carbpol.2013.05.079

Yeng, C. M., Husseinsyah, S., and Ting, S. S. (2015). "A comparative study of different crosslinking agent-modified chitosan/corn cob biocomposite films," *Polym. Bull.* 72(4), 791-808. DOI: 10.1007/s00289-015-1305-8

Zailuddin, N. L. I., Husseinsyah, S., Hahary, F. N., and Ismail, H. (2015). "Treatment of oil palm empty fruit bunch regenerated cellulose biocomposite films using methacrylic acid," *BioResources* 11(1), 873-885. DOI: 10.15376/biores.11.1.873-885

Zhang, H., Wu, J., Zhang, J., and He, J. (2005). "1-Allyl-3-methylimidazolium chloride room temperature ionic liquid: A new and powerful nonderivatizing solvent for cellulose," *Macromolecules* 38(20), 8272-8277. DOI: 10.1021/ma0505676

Zhang, J., Zhang, H., Wu, J., Zhang, J., He, J., and Xiang, J. (2010). "NMR spectroscopic studies of cellobiose solvation in EmimAc aimed to understand the dissolution mechanism of cellulose in ionic liquids," *Phys. Chem. Chem. Phys.* 12(8), 1941-1947. DOI: 10.1039/b920446f

Zhu, S., Wu, Y., Chen, Q., Yu, Z., Wang, C., Jin, S., and Wu, G. (2006). "Dissolution of cellulose with ionic liquids and its application: A mini-review," *Green Chem.* 8(4), 325-327. DOI: 10.1039/b601395c

Zimmermann, T., Bordeanu, N., and Strub, E. (2010). "Properties of nanofibrillated cellulose from different raw materials and its reinforcement potential," *Carbohydr. Polym.* 79(4), 1086-1093. DOI: 10.1016/j.carbpol.2009.10.045

Article submitted: March 19, 2016; Peer review completed: August 6, 2016; Revised version received and accepted: August 14, 2016; Published: August 30, 2016.
DOI: 10.15376/biores.11.4.8739-8755